ELSEVIER

Journal of Power Sources 86 (2000) 289–293

JOURNAL OF POWER SOURCES

www.elsevier.com/locate/jpowsour

Effects of flow rate and starvation of reactant gases on the performance of phosphoric acid fuel cells

Rak-Hyun Song *, Chang-Soo Kim, Dong Ryul Shin

Korea Institute of Energy Research, PO Box 103, Yusong, Taejon 305-600, South Korea

Accepted 26 October 1999

Abstract

Effects of reactant gas flow rates and starvation on the performance of phosphoric acid fuel cells were studied using single cells. As the reactant gas flow rates of single cell increased, the performance of the cell increased, and then remained constant. The optimum flow rates of hydrogen, oxygen and air under cell operating condition of 150 mA/cm^2 at 190°C were found to be 5 cc/min · cm^2, 5 cc/min · cm^2, and 15 cc/min · cm^2 at 1 atm and room temperature, respectively. The open circuit voltage of the single cell decreased with increasing oxygen flow rate at constant hydrogen flow rate, which is attributed to the increased gas cross-over rate. When the reactant gases were again supplied to the cell after gas starvation, the cell voltage losses were found to be about 5 mV in the case of hydrogen starvation and about 1 mV for oxygen starvation, and the voltage loss was independent of gas starvation time. These results were discussed from the electrochemical viewpoint of the cell.

Keywords: Gas flow rate; Gas starvation; Phosphoric acid fuel cell performance

1. Introduction

The fuel cell has been investigated as a new energy technology, because the fuel cells produce electricity directly from hydrogen fuel with an oxidant by electrochemical reaction at high efficiency, and offer a clean and pollution-free technology [1–3]. There are several types of fuel cells and these are usually classified into phosphoric acid, molten carbonate and solid oxide types. Amongst these fuel cells, the phosphoric acid fuel cell (PAFC) represents the technology most advanced in research and in development for practical use. The phosphoric acid fuel cell is fabricated by stacking single cells that consist of electrodes, electrolyte matrix, and bipolar plate. This produces electricity when the appropriate reactant gases are supplied to the cell.

When the fuel cell is operated, the reactant gases should be supplied at differing rates in accordance with the quantity of electricity required. If only small amounts of reactant gas are supplied to the cell, the cell performance would decrease. If much larger amounts of reactant gas are supplied, the performance may increase, although the cells will waste much fuel. Moreover, excess amounts of reactant gas may bring about irreversible loss of performance due to large pressure differences in the cell [4]. Therefore, the optimum rate of reactant gases should be determined in order to operate the fuel cell at high efficiency. Also, during the operation of the fuel cell, unexpected cessation of the reactant gas supply may occur, which induces an emergency state for the fuel cell system. Surprisingly, there are few studies of gas starvation, and its influence on the fuel cell performance is not clear, although changes of the electrode potential have been reported [5].

In this study, we examined the performance characteristics in accordance with the amount of hydrogen, oxygen, and air supplied as the reactant gases by using single cells. We also investigated the effects of the starvation of reactant gas on the performance of PAFC cells.

2. Experimental

The single cell consists of electrodes, electrolyte matrix, bipolar plate and current collectors. The electrode is composed of a carbon paper as electrode support and Pt/C powder as catalyst layer. The carbon paper was impregnated in a waterproofing solution for 30 s, so as to prevent the blockage of pores from the inflow of electrolyte solu-

* Corresponding author Tel.: +82-42-860-3578; fax: +82-42-860-3739; e-mail: rhsong@kier.re.kr

0378-7753/00/$ - see front matter
PII: S0378-7753(99)00450-4

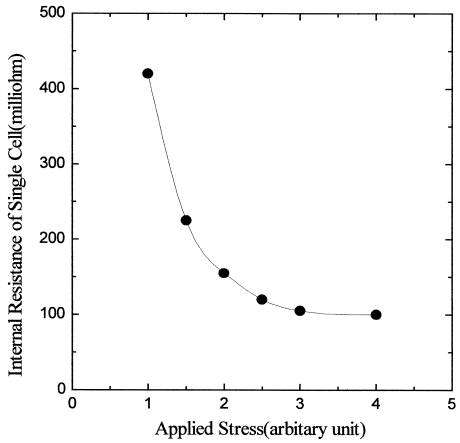

Fig. 1. Dependence of internal resistance of single cell on applied stress.

tion or water, and dried in air for 24 h, and then waterproofed by heating in air at 375°C for 30 min. The electrode catalyst layer, with a thickness of 0.2 mm, was manufactured by mixing Pt/C powder, polytetrafluoroethylene (PTFE) emulsion and solvent. Then the electrode support and catalyst layer was cold-pressed, dried at 100°C and sintered at 350°C in a N_2 atmosphere, so as to inhibit the generation of cracks in the catalyst layer and the detachment of the catalyst layer from the support body.

The electrolyte matrix was prepared from SiC powder. The SiC powder and PTFE emulsion were mixed in a solution to make the SiC slurry. The SiC slurry was coated on the cathode by using a doctor blade machine and then the coated matrix was sintered at 300°C for 30 min. The electrolyte was 105 wt.% H_3PO_4. Graphite was used as the bipolar plate material because carbon is stable at the fuel cell operating temperature of 190°C; its electric conductivity is good and its reactivity with phosphoric acid is low. The bipolar plate was machined into a ribbed shape to give a good distribution of reactant gases. A copper plate was used as current collector.

The single cell was fabricated by attaching the anode to the matrix-coated cathode. Before making the single cell, the matrix-coated cathode was impregnated with phosphoric acid at 130°C. After placing the bipolar plate and the current collector on the layered anode/matrix/cathode, the steel compression plates were attached at both sides. Then the single cell was compressed until a constant electric resistance was obtained by measuring the internal resistance of cell. Fig. 1 shows the internal resistance of the single cell at room temperature as a function of applied stress during the cell assembly. With increasing applied stress, the cell internal resistance decreased rapidly and maintained a constant value, which is attributed to the decreased contact resistance across the current collector, bipolar plate, catalyst layer, and electrolyte layer inside the cell. When the electrical contact is made satisfactory, the internal resistance maintains a constant value. Therefore, we manufactured single cells by compressing to this criterion. The effective electrode area of the single cell was 10 cm^2.

For performance testing of single cells, we constructed an equipment for performance measurements that could control the flow rate of hydrogen, oxygen and air. A variable electrical load was connected to the current collectors. The cell tests were carried out at 190°C with reactant gas supplied and with the variable load. Pure hydrogen was used as a fuel on the anode side, and oxygen or air as an oxidant on the cathode side. Flow rates of hydrogen and oxygen were in the range of 10 to 70 cc/min, and the flow rate of air was in the range of 10 to 250 cc/min.

In order to investigate the cell performance change during starvation of reactant gases, the cell was operated at a constant current density of 150 mA/cm^2 for 10 h and then the gases supplied to the cell were shut off for 1 to 1000 min. After gas starvation, the cell was operated again at the constant current density of 150 mA/cm^2 whilst re-supplying reactant gas.

3. Results and discussion

3.1. Effect of supplied gas flow rate on single cell performance

Fig. 2 shows the polarization curves of single cell for various oxygen flow rates at a constant hydrogen flow rate of 50 cc/min. The cell performance decreased with decreasing oxygen flow rate. When the oxygen flow rate was below 10 cc/min, a limiting current density of about 150 mA/cm^2 was apparent in the polarization curve of single cell. In the case of hydrogen and air, similar tendencies were also observed.

According to Bockris and Srinivasan [6], the low current density region of single cell polarization curves is determined by activation process, which is characterized

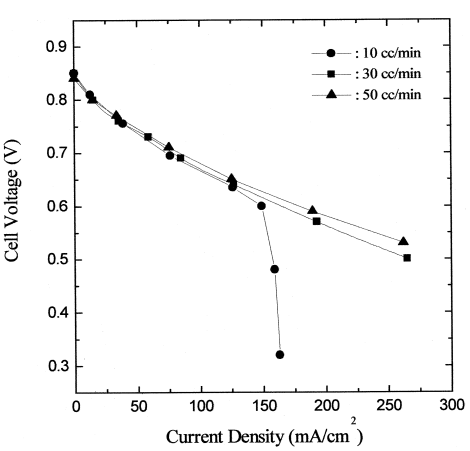

Fig. 2. Characteristics of cell performance for various oxygen flow rates under constant hydrogen flow rate of 50 cc/min.

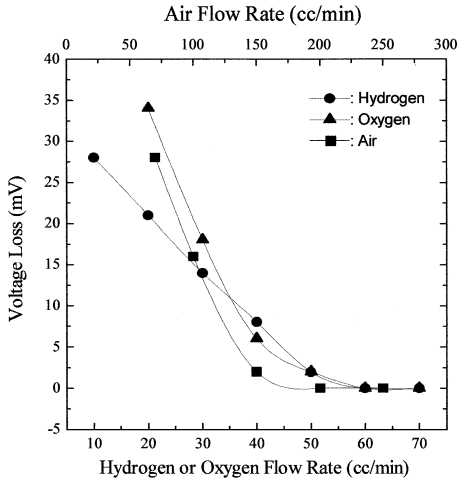

Fig. 3. Effect of gas flow rates on voltage loss of single cell at a current density of 150 mA/cm^2. Hydrogen (lower *x*-axis, left *y*-axis), oxygen (lower *x*-axis, left *y*-axis), air (top *x*-axis, left *y*-axis).

by the exchange current density and Tafel slope of cell. In the middle range of current densities, the polarization curve depends on the internal resistance and tends to linearity. The high current density region is subject to concentration overvoltage, characterized by a limiting current density. The present results can be explained on this basis. In Fig. 2, the polarization curve in the low current density region did not change with decreasing oxygen flow rate. This means that the oxygen flow rate does not have a great effect on the activation process of the cell in the measured flow rate range because the activation process is related to the three-phase boundary structure and the reaction mechanism.

The internal resistance of single cells consists of the electrolyte resistance, electrode resistance, bipolar plate resistance and contact resistance of components. Therefore, a change of oxygen flow rate does not affect the internal resistance. On the other hand, the polarization curve in the high current density domain depended very much on the oxygen flow rate. In this region, the cell voltage decreased with decreasing oxygen flow rate, which originates from an increase of concentration overvoltage, caused by the deficiency of oxygen supply to the reaction site at the cathode. This explanation is also relevant in the case of hydrogen and air. In the polarization curve, when the current density increases, the electrical power from the cell also increases, but when a limiting current density occurs, cell voltage decreases rapidly. In other words, when the polarization curve of a single cell is controlled by activation and resistance overvoltages, the performance of the cell increases with increasing current density. On the contrary, the performance decreases slowly upon the appearance of concentration overvoltage, and when it is close to the limiting current density, its performance decreases abruptly. Therefore, to protect the cell from an occurrence of limiting current density, the reactant gases should be carefully monitored and adjusted.

To clarify the dependence of cell voltage on gas flow rate under practical PAFC operating condition of 150 mA/cm^2, the voltage losses of single cells were examined as a function of gas flow rate; the results are presented in Fig. 3. Voltage loss is defined as the difference between the maximum cell voltage obtainable by changing the flow rate, and the actual cell voltage at each flow rate. The voltage loss relates to the cell efficiency loss because the cell efficiency is proportional to the cell voltage [7]. The cell voltage loss decreased with increasing flow rates and then almost vanished above critical flow rates of 50 cc/min of oxygen and hydrogen, and 150 cc/min of air. This means that if the gas flow rate is higher than the critical flow rate for each gas, then excess flow rates waste the reactant gases. From Fig. 3, based on the electrode area of a single cell, the optimum flow rates are estimated to be 5 cc/min · cm^2 in oxygen and hydrogen, and 15 cc/min · cm^2 in air under cell a operating condition of 150 mA/cm^2; these values are required for producing good cell efficiency and performance.

Fig. 4 shows the effect the change of oxygen flow rate on open circuit voltage (OCV) of the single cell. The OCV decreased with increasing oxygen flow rate. From thermodynamic consideration, the OCV of fuel cell is described as follows:

$$E_{\mathrm{OCV}}(V) = E^{\mathrm{o}} + \frac{RT}{2F}\ln\left(\frac{P_{\mathrm{H_2}}}{P_{\mathrm{H_2O}}}\right) + \frac{RT}{2F}\ln\left(P_{\mathrm{O_2}}\right)^{\frac{1}{2}} \qquad (1)$$

where E^{o} is the standard reversible potential. From this equation, it is noted that the OCV of a single cell is dependent on the partial pressure of oxygen, hydrogen and water in the cell. As the flow rate increased, the measured gas pressure in the cathode increased from 1 to 1.01 atm. Assuming that there is no gas cross-over, from Eq. (1) and the change of gas pressure, the theoretical change of OCV is estimated to be about 1 mV in the range of oxygen flow

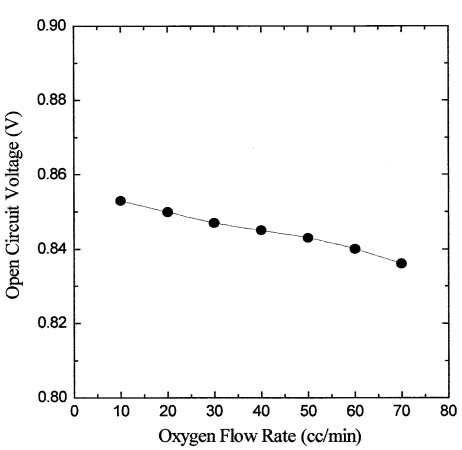

Fig. 4. Dependence of open circuit voltage of single cell on oxygen flow rate under constant hydrogen flow rate of 50 cc/min.

rates of 10 to 70 cc/min. The thermodynamic change in OCV calculated from the increment of the gas pressure is very small compared to the measured value of about 18 mV. Therefore, other reasons for the decrease of OCV should be considered. Gas cross-over may be responsible because the measured OCV is rather low compared to the theoretical OCV, 1.146 V.

Gas cross-over in single cell occurs through electrolyte, or gas leakage by incomplete sealing at the edge of the cell. The increased oxygen partial pressure at high flow rates induces pressure differences between the anode and the cathode sides, which may increase the gas cross-over rate. To confirm a gas cross-over effect, we measured the hydrogen content in the cathode. About 7% hydrogen was found. The hydrogen in the cathode reacts with oxygen to produce water due to the catalytic effect of platinum on the cathode and, thus, the measured hydrogen in the cathode is considered to be a result of hydrogen cross-over. Moreover, in the exit anode gas, water was observed, which means that oxygen gas cross-over occurred. Therefore, it seems to be reasonable to conclude that the decrease in OCV at high flow rates is due to the increased gas cross-over rate.

3.2. Effect of gas starvation on single cell performance

Fig. 5 shows the voltage loss of a single cell as a function of gas starvation time at a current density of 150 mA/cm^2. Voltage loss is defined as the difference in single cell voltages at 150 mA/cm^2 before gas starvation and after gas re-supply to the gas-starved cell. Voltage losses arising from hydrogen starvation showed high values of about 5 mV as compared to low values of about 1 mV under oxygen starvation. Also, cell voltage losses did not depend significantly on starvation times. Fig. 6 represents the polarization curves of half cells at the cathode and the anode, and for the single cell [6]. The present results of gas starvation can be explained on the basis of

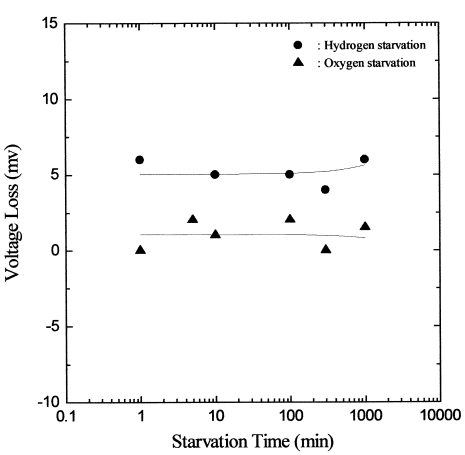

Fig. 5. Effects of starvation time of the reactant gases on the cell voltage loss.

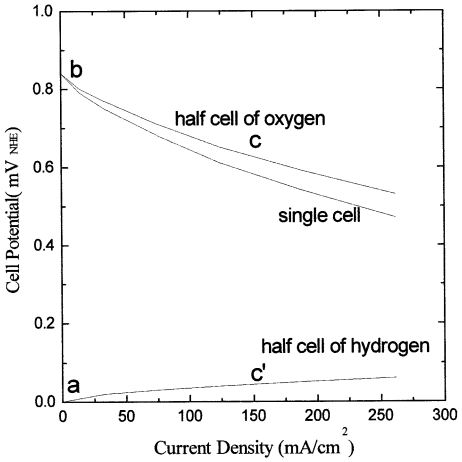

Fig. 6. Typical polarization curves of half cell and single cell in phosphoric acid fuel cell.

electrochemical polarization. When oxygen starvation occurs, the oxygen electrode potential moves from c to a and the hydrogen electrode potential moves from c′ to a because, during oxygen starvation, hydrogen was supplied continuously to the anode side of the single cell and the measured cell voltage rapidly approached zero. On the other hand, when hydrogen starvation occurs, the oxygen electrode potential moves from c to b and the hydrogen electrode potential moves from c′ to b because oxygen at the cathode was not depleted and the cell voltage dropped to zero in similar fashion.

In the same way, when oxygen is re-supplied after gas starvation, the oxygen electrode potential moves from a to c and hydrogen electrode potential moves from a to c′. On the other hand, when hydrogen re-supply occurs, the oxygen electrode potential moves from b to c and hydrogen electrode potential moves from b to c′. As a result, when a state of hydrogen starvation occurs, both oxygen and hydrogen electrodes are subject to the corrosion potential of carbon, which is recognized as one of the cell performance degradation factors [8]. However, although carbon corrosion increases with increasing starvation time, the cell voltage loss was independent of the hydrogen starvation time. Therefore, under hydrogen starvation, electrode corrosion is not considered to be a principal factor.

During reactant gas starvation, the three-phase boundary area of electrode/electrolyte/gas may be altered due to its dependence on the electrode potential and the gas partial pressure [9]. The experimental results for oxygen starvation may be evidence of such a change of the three-boundary area. During oxygen starvation, both the hydrogen electrode potential and the oxygen electrode potential move to lower values and, thus, electrode corrosion does not occur at this potential. Nevertheless, oxygen starvation results in cell performance loss. This means that when oxygen is depleted, the three-phase boundary area probably decreases due to electrolyte flooding.

Practically, in the case of reactant gas starvation, the voltage of the single cell moved from a constant value to zero rapidly. The transition time to zero was approximately 60 s for hydrogen starvation and 20 s for oxygen starvation. Upon re-supplying the gases after gas starvation, the voltage rose again to a constant value. The transition times returning to constant voltage were 120 s for hydrogen re-supply and 50 s for oxygen re-supply. The transition time for cell voltage, in the case of hydrogen starvation, is longer than that for oxygen starvation although the shorter transition times for hydrogen starvation was expected, since a greater amount of hydrogen was required during the stoichiometric cell reaction. This means that a change of the three-phase boundary area must have occurred during gas starvation. Thus, it seems to be reasonable to conclude that the cell performance loss during gas starvation is due to the decreased three-phase boundary area, and that this performance loss is irreversible. In the present work, it is not clear whether carbon corrosion has an effect on the performance loss of the gas-starved cell.

4. Conclusions

The effects of the flow rate and starvation of reactant gases on cell performance of PAFCs were studied and the following conclusions were drawn. The concentration overvoltage in polarization curves increased with decreasing hydrogen, oxygen, and air flow rates. Below critical flow rates of gases, the cell performance decreased considerably to the extent that a limiting current density appeared. The optimum flow rates of oxygen, hydrogen and air at a cell operating condition of 150 mA/cm^2 were found to be 5 $cc/min\ cm^2$, 5 $cc/min\ cm^2$, and 15 $cc/min \cdot cm^2$, respectively. As the oxygen flow rate increases, the measured OCV of the single cell decreased much more than the theoretical OCV calculated from a thermodynamic consideration of oxygen partial pressure; this is attributed to the increased gas cross-over rate. When the reactant gases were re-supplied to the cell after gas starvation, the voltage losses of the fuel cell were found to be about 5 mV in the case of hydrogen starvation, and about 1 mV in the case of oxygen starvation, which is considered to be related to a change in the three-phase boundary structure.

Acknowledgements

This work was supported by the Ministry of Commerce, Industry and Energy, and Ministry of Science and Technology, Korea.

References

[1] A.J. Appleby, Assessment of research needs for advanced fuel cells, Energy Inter. J. 11 (1/2) (1986) 13–94.
[2] R.-H. Song, D.R. Shin, C.-S. Kim, New method of electrode fabrication for phosphoric acid fuel cell, Int. J. Hydrogen Energy 23 (11) (1998) 1049–1053.
[3] R.-H. Song, D.R. Shin, C.-S. Kim, S.-H. Choi, Fabrication and performance characteristics of 10 kW phosphoric acid fuel cell, J. New Mat. Electrochem. Syst. 12 (1999) 131–135.
[4] A. Kaufman, P. Terry, Phosphoric Acid Fuel Cell Development, Engelhard Min. and Chem., Technical Report, New Jersey, Sep. 1980.
[5] K. Mitsuda, T. Murahashi, Air and fuel starvation of phosphoric acid fuel cells: a study using a single cell with multi-reference electrodes, J. Appl. Electrochem. 21 (1991) 524–530.
[6] J. O'M. Bockris, S. Srinivasan, Fuel Cells: Their Electrochemistry, McGraw-Hill Book, 1969, pp. 176–229.
[7] R. Anahara, Fuel cell systems, in: L.J.M.J. Blomen, M.N. Mugerwa (Eds.), Plenum, New York, 1993, pp. 285–287.
[8] K. Kinoshita, Carbon: Electrochemical and Physicochemical Properties, Wiley, 1987, pp. 293–387.
[9] D.R. Crow, Principles and Applications of Electrochemistry, Chapman & Hall, 1981, pp. 214–218.